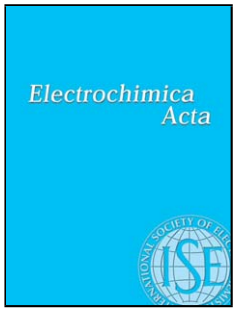

Title: Formation of a robust and stable film comprising ionic liquid and polyoxometalate on glassy carbon electrode modified with multiwall carbon nanotubes: toward sensitive and fast detection of hydrogen peroxide and iodate

Authors: Behzad Haghighi, Hassan Hamidi, Lo Gorton

PII: S0013-4686(10)00443-3
DOI: doi:10.1016/j.electacta.2010.03.041
Reference: EA 15623

To appear in: *Electrochimica Acta*

Received date: 15-10-2009
Revised date: 8-3-2010
Accepted date: 13-3-2010

Please cite this article as: B. Haghighi, H. Hamidi, L. Gorton, Formation of a robust and stable film comprising ionic liquid and polyoxometalate on glassy carbon electrode modified with multiwall carbon nanotubes: toward sensitive and fast detection of hydrogen peroxide and iodate, *Electrochimica Acta* (2008), doi:10.1016/j.electacta.2010.03.041

Formation of a robust and stable film comprising ionic liquid and polyoxometalate on glassy carbon electrode modified with multiwall carbon nanotubes: toward sensitive and fast detection of hydrogen peroxide and iodate

Behzad Haghighi[*,a], Hassan Hamidi [a], Lo Gorton [b]

[a] *Department of Chemistry, Institute for Advanced Studies in Basic Sciences, P.O. Box 45195 – 1159, Gava Zang, Zanjan, Iran.*

[b] *Institute of Chemistry, Lund Universit, P.O. Box 124, S-221 00 Lund, Sweden*

Abstract

A robust and stable film comprising *n*-octylpyridinum hexafluorophosphate ($[C_8Py][PF_6]$) and 1:12 phosphomolybdic acid (PMo_{12}) was prepared on glassy carbon electrodes modified with multiwall carbon nanotubes (GCE/MWCNTs) by dip-coating. The cyclic voltammograms of the GCE/MWCNTs/$[C_8Py][PF_6]$-PMo_{12} showed three well-defined pairs of redox peaks due to the PMo_{12} system. The surface coverage for the immobilized PMo_{12} and the average values of the electron transfer rate constant for there pairs of redox peaks were evaluated. The GCE/MWCNTs/$[C_8Py][PF_6]$-PMo_{12} showed great electrocatalytic activity toward the reduction of H_2O_2 and iodate. The kinetic parameters of the catalytic reduction of hydrogen peroxide and iodate at the electrode surface and analytical features of the sensor for amperometric determination of hydrogen peroxide and iodate were evaluated.

[*] Corresponding author. Tel: +98 241 4153 126, Fax: +98 2414153 232
E-mail address: haghighi@iasbs.ac.ir (B. Haghighi)

Keywords: Phosphomolybdic acid; Ionic liquid; Modified electrode; H_2O_2; Iodate.

1. Introduction

The diversity of research fields connected to the chemistry of polyoxometalates (POMs) is significant and includes their application in many areas such as analytical chemistry, structural chemistry, surface chemistry, electrochemistry, photochemistry and medicine [1-3]. The POMs have the ability to proceed in multiple, consecutive, and reversible multielectron charge transfer reactions which are the basis for many catalysis processes without decomposition to the mixed-valence species [4]. During the past few years, significant developments on electrode modification by POMs have taken place aiming at improving the reactivity and selectivity of electrochemical sensors. Several successful strategies have been developed to fabricate chemically modified electrodes based on POMs as electrocatalysts, including electrochemical deposition [5-7], layer-by-layer deposition [8, 9], adsorption [10-12], self assembly monolayers [13, 14], Langmuir-Blodgett [9, 12] and sol-gel films[15, 16], entrapment as a dopant in conductive polymeric matrices[17-19], in carbon ceramic electrode [20] and in carbon paste electrode [21-24]. Most of the methods mentioned above achieved great success, but some of them suffered from some shortcomings including poor long-term stability, complicated preparation process and so on. Therefore, the research for simple and convenient methods for immobilization of polyoxometalate still remains a challenge.

Since the first discovery of carbon nanotubes (CNTs) [25], there has been an enormous interest in exploring and exploiting their unique properties [26]. One promising application of CNTs is their use in chemical sensors and nanoscale electronic device [27, 28]. The key advantages of carbon nanotube modified electrodes are their small diameter but long length, their electro-activity which appears to be as good or

better than any of the other carbon based electrodes and their high surface area [28]. Combination of carbon nanotubes and polyoxometalates gives the opportunity to increase functionality and performance of POMs as an electrocatalyst in the area of chemically modified electrodes [9, 29-36].

Ionic liquids (ILs) belong to a special group of electrolytes consisting only of ions and are free of any molecular solvent. A typical IL that is stable in air and water is based on combining of organic cations (e.g. *n*-alkylpyridinium, *n*,*n*-dialkylimidazolium) with a variety of anions (e.g. Cl^-, Br^-, I^-, $AlCl_4^-$, NO_3^-, PF_6^-, BF_4^-, CF_3^-, SO_3^-, CF_3COO^-, $(CF_3SO_2)_2N^-$ (Tf_2N^-) and $(C_2F_5SO_2)_2N^-$ (Pf_2N^-). In recent years, ILs have been widely used in the fields of electrochemistry and electroanalysis [37-39]. Ionic liquids have demonstrated the distinct advantages such as high chemical and thermal stability, relatively high ionic conductivity, negligible vapor pressure and wide electrochemical windows [38, 39]. ILs can be employed not only as the supporting electrolyte but also as the modified materials. Imidazolium and pyridinium salts are the most important classes of ILs, and have accordingly received much attention. Considerable progresses have been made in application of immidazolium based ILs in the modification of electrodes either as a physically adsorbed film [40, 41] or in conjunction with carbon paste as a bulk-modified electrode [24, 42-44]. Since the pioneering work of Maleki's group [45] based on the use of the $[C_8Py][PF_6]$ as the binder, much effort has been devoted to fabricate chemically modified electrode using pyridinium based IL [46-50]. Several works have reported improved electrochemical properties that were exhibited by the POMs when ionic liquids used as a solvent or a modifier in construction of chemically modified electrodes[21, 24, 40, 48, 51-54].

In the present paper, a new strategy was applied to prepare a robust and stable film comprising $[C_8Py][PF_6]$ and PMo_{12} on GCE/MWCNTs by dip-coating. The attractive mechanical and electrical characteristics of carbon nanostructures were combined with

the unique properties of ionic liquids and polyoxometalates using the proposed strategy. The electrochemical properties of the GCE/MWCNTs/$[C_8Py][PF_6]$-PMo_{12} and its electrocatalytic activity toward hydrogen peroxide and iodate reduction were studied. The Kinetic parameters of the catalytic reduction of hydrogen peroxide and iodate at the electrode surface and analytical features of the sensor for amperometric determination of hydrogen peroxide and iodate were evaluated.

2. Experimental

2.1. Reagents and chemicals

High quality grade chemicals were used without further treatment. 1:12 phosphomolybdic acid $[H_3(PMo_{12}O_{40})\cdot xH_2O]$ (PMo_{12}), *n*-octyl iodide, pyridine, ammonium hexafluorophosphate, graphite powder (particle size < 0.1 mm), sulfuric acid, sodium hydroxide, acetonitrile, dimethylformamide, hydrogen peroxide and sodium iodate were obtained from Merck (Darmstadt, Germany). *n*-Octylpyridinium hexafluorophosphate ($[C_8Py][PF_6]$) were prepared according to the method reported previously [48, 55]. Multi-wall carbon nanotubes (MWCNTs, 95% purity, OD = 10-30 nm, ID = 5-10 nm and length = 0.5-500 μm) were obtained from Aldrich, (Steinheim, Germany). The MWCNTs were purified according to the method reported previously [27]. In brief, 50 mg of carbon nanotubes were dispersed in 60 mL of 2.2 M HNO_3 and ultrasonicated for 30 min and the suspension was then kept at room temperature for 20 h. The MWCNTs were then filtered, washed with distilled water to neutrality and dried at 37 °C in an oven.

H_2SO_4 solutions (0.5 M) of various pHs (1.03-3.04) were prepared by mixing a stock H_2SO_4 solution with appropriate amounts of NaOH solution. Deionized, triply distilled water was used for preparing all solutions and diluting them.

2.2. Apparatus

Cyclic voltammetry (CV) and amperometric studies were performed using an Autolab potentiostat-galvanostat model PGSTAT30 (Utrecht, The Netherlands) with a conventional three-electrode set-up in which GCE/MWCNTs/$[C_8Py][PF_6]$-PMo_{12}, an $Ag|AgCl|KCl_{sat}$ electrode and a platinum rod served as the working, reference and auxiliary electrodes, respectively. The working potential was applied to the GCE/MWCNTs/IL-PMo_{12} in the standard way using the potentiostat and the output signal was acquired by Autolab GPES software. Electrochemical impedance spectroscopy (EIS) experiments were carried out in phosphate buffer solution (0.1 M and pH of 7) containing 5 mM $[Fe(CN)_6]^{4-/3-}$ at the formal potential of the system. The frequency was ranged from 0.1 Hz to 100,000 Hz with signal amplitude of 10 mV. Scanning electron microscopy (SEM) was performed with a Philips instrument, Model X-30. A Metrohm 691 pH meter was used for pH adjustments. All measurements were performed at room temperature.

2.3. Fabrication of GCE/MWCNTs/$[C_8Py][PF_6]$-PMo_{12}

The surface of a glassy carbon electrode (Sigradur K, HTW Hochtemperature Werkstoffe GmbH, Thierhaupten, Germany) was polished successively with 0.3 and 0.1 μm alumina paste (Struers, Copenhagen, Denmark) to obtain a mirror finish and then cleaned in ethanol and water under ultrasonication. One milligram of purified MWCNTs were dispersed in 1 mL of *n*,*n*-dimethylformamide (DMF) with ultrasonic agitation for an hour to achieve a well dispersed suspension. 5 μL of the prepared MWCNTs suspension were placed on the surface of a GC electrode and dried in an oven at 50°C. The glassy carbon electrode modified with multiwall carbon nanotubes (GCE/MWCNTs) was then immersed in a acetonitrile solution containing 25 mg mL^{-1} $[C_8Py][PF_6]$ and 0.5 mg mL^{-1} PMo_{12} for 1 min. The modified GCE with MWCNTs,

$[C_8Py][PF_6]$ and PMo_{12} (GCE/MWCNTs/$[C_8Py][PF_6]$-PMo_{12}) was allowed to dry in air and ready for use. For comparison, GCE/$[C_8Py][PF_6]$-PMo_{12}, GCE/MWCNTs/PMo_{12} and GCE/MWCNTs/$[C_8Py][PF_6]$ were prepared through a similar procedure.

The apparent surface area (A) of the bare GCE and GCE/MWCNTs was estimated using CV. The CV experiments were performed in a 5 mM $K_3[Fe(CN)_6]$ in 0.1 M KCl solution at various scan rates using both electrodes. A straight line for a plot of peak currents (i_p) versus scan rates ($v^{1/2}$) could be obtained according to the equation of $i_p = 2.69 \times 10^5 n^{2/3} A D^{1/2} v^{1/2} c_o$ [56]. The estimated values of A, calculated from the slope of the straight line, for the bare GCE and GCE/MWCNTs were 0.076 and 0.116 cm^2, respectively.

3. Results and Discussion

The morphologies of the GCE/MWCNTs, GCE/MWCNTs/$[C_8Py][PF_6]$ and GCE/MWCNTs/$[C_8Py][PF_6]$-PMo_{12} were investigated with SEM. As shown in Fig. 1a, MWCNTs are discernible after its suspension is cast on the GCE. The surface of the GCE/MWCNTs/$[C_8Py][PF_6]$ is quite even, highly uniform and the MWCNTs are indiscernible, which can be attributed to the binding and blanketing effect of $[C_8Py][PF_6]$ (Fig. 1b). However, when $[C_8Py][PF_6]$-PMo_{12} is placed on GCE/MWCNTs a very fine cracks were observed (Fig. 1c).

Potassium ferricyanide (5 mM in 0.1 M KCl solution) was selected as a probe to evaluate the performance of the GCE, GCE/MWCNTs and GCE/MWCNTs/$[C_8Py][PF_6]$ using CV. A pair of well-defined redox peaks with a peak-to-peak separation (ΔE_p) of 97 mV was observed at the bare GCE (Fig. 2A-a). After modification of the GCE with MWCNTs the peak current increased, obviously and the ΔE_p decreased to 86 mV (Fig. 2A-b), showing the enhancement in the rate of electron transfer rate at the GCE/MWCNTs surface. While at the GCE/MWCNTs/$[C_8Py][PF_6]$

(Fig. 2A-c), the peak current further increased and the ΔE_p further decreased (75 mV), suggesting the MWCNTs/$[C_8Py][PF_6]$ film on GCE can further enhance the rate of electron transfer. Additionally, the background current at the GCE/MWCNTs electrode was larger than that of the bare GCE due to larger charging current and higher surface area. While the background current of the GCE/MWCNTs/$[C_8Py][PF_6]$ was smaller than that of the GCE/MWCNTs but still remained larger than that of the bare GCE. This means the ionic liquid can reduce the background current of modified electrode caused by carbon nanotubes.

EIS experiments were also done to investigate the effect of modification process on the impedance of the electrode surface. Figure 2B shows the Nyquist plots (Z_{im} vs. Z_{re}) of the EIS experiments for the bare GCE, GCE/MWCNTs and GCE/MWCNTs/$[C_8Py][PF_6]$. The charge-transfer resistance (R_{ct}) value for the $Fe(CN)_6]^{4-/3-}$ couple (5 mM in 0.1 M phosphate buffer pH of 7) at the bare GCE (2B-d, 816 Ω) was much higher than that of GCE/MWCNTs (2B-e, 186 Ω) and GCE/MWCNTs/$[C_8Py][PF_6]$ (2B-f, 145 Ω), which indicated that the modification of GCE with MWCNTs and further with $[C_8Py][PF_6]$ enhanced the rate of electron transfer.

3.1. Cyclic voltammetric studies of GCE/MWCNTs/$[C_8Py][PF_6]$-PMo_{12}

Figure 3 presents the cyclic voltammograms of GCE/MWCNTs/$[C_8Py][PF_6]$-PMo_{12}, GCE/MWCNTs/$[C_8Py][PF_6]$, GCE/MWCNTs/PMo_{12} and GCE/$[C_8Py][PF_6]$-PMo_{12} in a 0.5 M H_2SO_4 solution. As shown in Figs. 3a and 3c, three reversible pairs of redox peaks in the potential range +0.5 to -0.15 V vs. Ag|AgCl|KCl_{sat} are observed for GCE/MWCNTs/$[C_8Py][PF_6]$-PMo_{12} and GCE/MWCNTs/PMo_{12} and no clear redox peaks for GCE/$[C_8Py][PF_6]$-PMo_{12} (Fig. 3d). The cyclic voltammogram of GCE/MWCNTs/$[C_8Py][PF_6]$ showed no redox peaks (Fig. 3b). Three pairs of redox

peaks i.e. I-I′, II-II′ and III-III′ corresponded to the oxidation and reduction of PMo_{12} through two-, four- and six-electron processes, respectively [8, 9, 19, 48, 57, 58]. The formal potentials ($E^{o'}=1/2(E_{pa}+E_{pc})$, the mean value of the anodic and cathodic peak potentials [56]), peak separations ($\Delta E_p=E_{pa}-E_{pc}$) and current densities for the recorded CVs are summarized in Table 1. The observed electrochemical characteristics were comparable or even better than those obtained for PMo_{12} modified MWCNTs electrodes which did not contain ionic liquid [36, 58].

GCE/MWCNTs/PMo_{12} (Fig. 3c) in comparison with GCE/$[C_8Py][PF_6]$-PMo_{12} (Fig. 3d) showed higher current density and a lower ΔE_p due to the high surface area and the catalytic effect of carbon nanotubes. In contrast GCE/MWCNTs/$[C_8Py][PF_6]$-PMo_{12} (Fig. 3a) with regard to GCE/MWCNTs/PMo_{12} (Fig. 3c) showed a further increase in current density and a slightly decrease in ΔE_p which implies that the rate of electron transfer is faster due to the synergic effect of MWCNTs and $[C_8Py][PF_6]$.

Figure 4a shows the cyclic voltammograms of GCE/MWCNTs/$[C_8Py][PF_6]$-PMo_{12} in 0.5 M H_2SO_4 solution at different scan rates (v). The results showed (Fig. 4b) the peak current density (j_p) for the three pairs of redox peaks increased linearly with v between 10 and 900 mV s^{-1} ($r^2_{I-I'}=0.9997$, $r^2_{II-II'}=0.9986$ and $r^2_{III-III'}=0.9988$) which revealed a surface-limited redox process. Moreover, the anodic peak current densities were almost the same as the corresponding cathodic peak current densities. At scan rates higher than 900 mV s^{-1} (Fig. 4c), plots of j_p versus $v^{1/2}$ were linear ($r^2_{I-I'}=0.9985$, $r^2_{II-II'}=0.9997$ and $r^2_{III-III'}=0.9849$), indicating a diffusion-controlled process, which might be related to the relatively slow diffusion of protons into the limited hydrated section of the electrode surface. The anodic and cathodic peak potentials (E_{pa} and E_{pc}) and consequently the ΔE_p were almost constant for scan rates lower than 800 mV s^{-1},

suggesting facile charge transfer kinetics over this range of scan rate, but at the higher scan rates (v > 800 mVs^{-1}) ΔE_p increased.

Laviron reported [59] that the transfer coefficient, α, and the electron transfer rate constant, k_s, can be deduced experimentally by measuring the variation of the peak potentials at different scan rates, when ΔE_p is smaller than 200/n mV and α ranges from 0.3 to 0.7. Laviron provided several groups of data corresponding to m^{-1} ($m = RTk_s/nFv$, where n, F, R and T have their usual meanings) and $n\Delta E_p$. He also pointed out that the relative error on k_s is at the most about 6% if a relationship for α = 0.5 was used. The values of m^{-1} were obtained by introducing the values of $n\Delta E_p$ into the regression equation, which was deduced from the data provided by Laviron and then k_s was calculated. The average values of k_s for there redox pairs I-I', II-II' and III-III' are 53.8 (± 0.8), 51.8 (± 0.6), 51.8 (± 1.2) s^{-1}, respectively assuming n = 2 for each pair. These high values for k_s indicate that PMo_{12} behaves as an excellent electron transfer mediator in the combined MWCNTs and $[C_8Py][PF_6]$ matrix in comparison with PMo_{12} modified carbon ionic liquid electrode [48] and glassy carbon electrode modified with carbon nanotubes and $SiMo_{12}$ [35].

The surface concentration (Γ_c) of electroactive species in GCE/MWCNTs/$[C_8Py][PF_6]$-PMo_{12} was evaluated from the slope of I_p versus v according to the equation 1 [49] derived for a reversible surface redox reaction:

$$I_p = \frac{n^2F^2Av\Gamma_c}{4RT} \quad (1)$$

in which A is the effective surface area (0.116 cm^2) and the other symbols have their usual meanings. The average value of Γ_c for all three pairs of redox peaks is 5.94 × 10^{-9} mol cm^{-2} for n = 2 and v < 900 mV s^{-1}.

The effect of pH on the electrochemical behavior of GCE/MWCNTs/$[C_8Py][PF_6]$-PMo_{12} was also studied at different pHs. As shown in Figure 5 both the reduction and

the oxidation peak potentials of the PMo_{12} redox couples shift to more negative potentials with increasing pH and the peak current densities decrease, similar to those results reported previously [4, 8, 48, 60]. The plots of $E_{1/2}$ versus pH ranging from 1.03 to 3.04 are all linear ($r^2 > 0.999$) for three observed peaks (Fig. 5 inset). The calculated slopes for I- I′, II-II′ and III-III′ redox pairs are -60, -78 and -63 mV pH^{-1} at 25 °C, respectively which are close to the theoretical value of -59 mV pH^{-1} for a $2e^-/2H^+$ redox process. Reduction of PMo_{12} in GCE/MWCNTs/$[C_8Py][PF_6]$-PMo_{12} is accompanied by the uptake of protons from solution to the hydrated electroactive section of the electrode surface to maintain charge neutrality. Therefore, the shift of $E_{1/2}$ to more negative potential with increasing pH can be elucidated using the Nernst equation [61] and also the decrease of the peak current density can be explained by a slower penetration of protons to GCE/MWCNTs/$[C_8Py][PF_6]$-PMo_{12} with increasing pH.

The storage stability of the GCE/MWCNTs/$[C_8Py][PF_6]$-PMo_{12} was examined using CV everyday over a period of 5 days by measuring the decrease in the voltammetric current density during potential cycling. The sensor was kept in a dry state in the room temperature between experiments. Recycling the potential for 500 times (100 cycles in each day) in the range between 0.5 and -0.2 V with a scan rate of 50 mVs^{-1} and in 0.5 M H_2SO_4 solution caused about 25% decrease in voltammetric current density after 5 days. The stability of the adsorbed PMo_{12} anions on the electrode surface could be due to the co-adsorption of relatively large counter ions on the surface, which inhibits the PMo_{12} anions dissolving from the electrode surfaces [40], while the cycling stability is less at the modified electrode without ionic liquid [58].

3.2. Electrocatalytic behavior of GCE/MWCNTs/$[C_8Py][PF_6]$-PMo_{12}

Many studies [8, 22, 23, 48, 57, 60, 62, 63] have shown that reduced POMs are capable of delivering electrons to other species, thus serving as powerful electron

reservoirs for multielectron reductions. In our studies, we found that GCE/MWCNTs/$[C_8Py][PF_6]$-PMo_{12} shows good electrocatalytic activity for the reduction of hydrogen peroxide and iodate.

3.2.1. Electrocatalytic reduction of hydrogen peroxide

Hydrogen peroxide in the troposphere is an important oxidant, producing sulfuric acid in the aqueous phase and is also thought to have some toxic effect on plants [64]. H_2O_2 is employed as an anti-bacterial agent and for sterilization in pharmaceutical and dairy industries, respectively. Peroxides is released in the environment from many industrial processes [65], produced during the processes of ozonation of the drinking water [66] and ozonation reaction in the air [67]. So, the analytical determination of hydrogen peroxide represents an important topic that has relevance pertaining to environmental, pharmaceutical, clinical and industrial research, as reported in many recent works [68-71].

Cyclic voltammetry was used to examine the electrocatalytic activity of the GCE/MWCNTs/$[C_8Py][PF_6]$-PMo_{12} toward electroreduction of hydrogen peroxide. It is known that electroreduction of hydrogen peroxide on a bare GCE requires a large overpotential. As shown in Figure 6 (inset), no response is observed for hydrogen peroxide on GCE/MWCNTs/$[C_8Py][PF_6]$ but GCE/MWCNTs/$[C_8Py][PF_6]$-PMo_{12} exhibits a good electrocatalytic activity towards hydrogen peroxide reduction (Fig. 6). The catalytic effect appeared on the reduction peak of the second redox pair (II-II′) of PMo_{12}, which corresponds to the reduction process from two-electron to four-electron reduced species.

The electrocatalytic reduction of H_2O_2 by GCE/MWCNTs/$[C_8Py][PF_6]$-PMo_{12} was also studied by chronoamperometry. Chronoamperometric results were obtained for various concentrations of H_2O_2 solution using GCE/MWCNTs/$[C_8Py][PF_6]$-PMo_{12} at a

working potential 100 mV vs. Ag|AgCl|KCl_{sat} (not shown). The current signals of GCE/MWCNTs/$[C_8Py][PF_6]$-PMo_{12} in the presence of H_2O_2 at various concentrations, which is expressed as the catalytic current (I_{cat}), and in the absence of H_2O_2, expressed as the limiting current (I_L), at various fixed times were then used to evaluate the rate constant for the chemical reaction between H_2O_2 and the redox sites of the GCE/MWCNTs/$[C_8Py][PF_6]$-PMo_{12} according to equation 2 [72]:

$$I_{cat}/I_L = \gamma^{1/2}[\pi^{1/2}\mathrm{erf}(\gamma^{1/2}) + \exp(-\gamma)/\gamma^{1/2}] \quad (2)$$

in which γ is the argument of the error function. In those cases $\gamma > 2$, the error function is almost equal to 1 and the equation 2 is simplified to:

$$I_{cat}/I_L = \gamma^{1/2}\pi^{1/2} = (kc_o t)^{1/2}\pi^{1/2} \quad (3)$$

where k, c_o, and t are the rate constant of the catalytic chemical reaction ($cm^3\ mol^{-1}\ s^{-1}$), the bulk concentration of H_2O_2 (mol cm^{-3}) and the extent a fixed time (s). Using the slope obtained from the plot of I_{cat}/I_L versus $t^{1/2}$, the value of k can be determined for a given concentration of H_2O_2. The mean value obtained for k in the concentration range between 0.4 and 1.4 mM is 3.7 (±0.3) × 10^8 $cm^3\ mol^{-1}\ s^{-1}$, which is much higher than the value (4.5 × 10^6 $cm^3\ mol^{-1}\ s^{-1}$) obtained for GCE/CNTs/$SiMo_{12}$ [35].

3.2.2. Electrocatalytic reduction of iodate

Iodine is an essential micronutrient, which is an essential part of the thyroid hormones that play an important role in the development of brain function and cell growth. Deficiency of iodine can result in a serious delay in neurologic development. Otherwise, an excess of iodine or iodide can produce goitre and hypothyroidism as well as hyperthyroidism [73]. Iodine is absorbed from foods, drugs and water. Potassium iodate has been extensively used for iodination of commercial table salts as a source of iodine for preventing of iodine deficiency disorders [74]. Therefore, the importance of

improved analytical methods for determination of iodate has received considerable attention [15, 20, 22, 48, 74, 75].

Preliminary investigations showed that a stable response for IO_3^- electroreduction could be achieved at a pH higher than 2.5, so studies were done at pH 2.5. Figure 7 shows cyclic voltammograms of GCE/MWCNTs/$[C_8Py][PF_6]$-PMo_{12} in the presence of IO_3^- at various concentrations. In the potential range between 0.35 and 0.05 V no electrocatalytic activity is observed for iodate reduction on GCE/MWCNTs/$[C_8Py][PF_6]$ (Fig.7, inset) but GCE/MWCNTs/$[C_8Py][PF_6]$-PMo_{12} exhibits good electrocatalytic activity towards iodate reduction. With increasing the concentration of iodate, the cathodic current density of the first pair of redox peaks (I-I′, see Fig. 3) enhanced and the corresponding oxidation current density decreases, but the second and third pairs of redox peaks i.e. II-II′ and III-III′ are almost unaffected by the addition of iodate. The catalytic effect observed on the reduction peak of the first redox pair (I-I′), which corresponds to the reduction process from the zero-electron to the two-electron reduced species.

The rate constant for the chemical reaction between iodate and the redox sites of the GCE/MWCNTs/$[C_8Py][PF_6]$-PMo_{12} was evaluated with chronoamperometry according to the method described above. The mean value obtained for k in the concentration range between 0.2 and 1.2 mM is 1.3 (±0.7) × 10^{12} cm^3 mol^{-1} s^{-1}, which is much higher than the value (7.26 × 10^6 cm^3 mol^{-1} s^{-1}) obtained for PMo_{12}-CILE in our previous work [48].

3.3. Amperometric determination of H_2O_2 and iodate

As shown above GCE/MWCNTs/$[C_8Py][PF_6]$-PMo_{12} has excellent mediation properties and ability for low potential amperometric measurement of iodate and hydrogen peroxide. Hydrodynamic voltammetry was performed for H_2O_2 and iodate

reduction to find the optimum working potential for amperometric measurement (not shown). Based on those results obtained, -0.1 and 0.0 V were selected as the optimum working potentials for H_2O_2 and iodate measurements, respectively. As shown in Figure 8a, for successive additions of H_2O_2 solution (0.02, 0.1 or 1 mM) well-defined responses are observed. Addition of a H_2O_2 solution causes a sharp increase in the current density with a response time of less than 2 s. The calibration curve for H_2O_2 determination is linear between 2×10^{-5} and 8×10^{-3} M with a correlation coefficient of 0.9999. The sensitivity and detection limit (signal to noise ratio = 3) of the sensor toward H_2O_2 detection are 73 μA mM^{-1} cm^{-2} and of 12 μM, respectively. Figure 8b shows a typical calibration plot for H_2O_2 determination and Figure 8c shows the amperometric response of GCE/MWCNTs/$[C_8Py][PF_6]$-PMo_{12} in the presence of 100 μM H_2O_2 over 30 min. As is obvious, the current signal is extremely stable and only a 3.5% decrease in current density was observed after 30 min. Also, amperometric experiments were carried out for IO_3^- determination. The calibration curve for IO_3^- detection was linear between 2×10^{-5} and 2×10^{-3} M and the sensitivity and the detection limit were 190 μA mM^{-1} cm^{-2} and of 15 μM, respectively. Electroanalytical characteristics of the proposed sensor towards hydrogen peroxide and iodate detection have been summarized and compared with those obtained using various modified electrodes in Table 2.

The operational stability of the sensor was examined by amperometric measurement every day over a period of 5 days using hydrogen peroxide. The sensor was kept in a dry state in the room temperature between experiments. Successive addition of 20 μM of hydrogen peroxide for 100 times (20 times in each day) caused the sensor lost about 60 % activity after 5 days, compared to the initial response.

4. Conclusions

A robust and stable film composed of an ionic liquid, $[C_8Py][PF_6]$, and a polyoxometalate, PMo_{12}, was prepared on glassy carbon electrodes modified with multiwall carbon nanotubes in 1 min by dip coating the electrode in an acetonitrile solution containing $[C_8Py][PF_6]$ and PMo_{12} . The high values obtained for the electron transfer and catalytic chemical reaction rate constants indicate that PMo_{12} behaved as an excellent electron transfer mediator in the combined MWCNTs and $[C_8Py][PF_6]$ matrix and showed that the attractive mechanical and electrical characteristics of carbon nanostructures combined with the unique properties of ionic liquids and polyoxometalates. The modified electrode showed the ability for hydrogen peroxide and iodate detection at reduced overpotential with many desirable properties including low detection limit, high sensitivity, short response time (< 2 s) and satisfactory linear concentration range. The main limitation of the proposed electrode, which is common in the most POM-modified electrodes, is the loss of its stability and catalytic activity at pH around 7 as polyoxometalates decompose normally very rapidly above pH 3. This drawback limits the utilization of POM-modified electrodes for the fabrication of biosensors where biological elements such as enzymes are used.

Acknowledgement

The authors acknowledge the Institute for Advanced Studies in Basic Science (IASBS, grant number G2009IASBS119), the Swedish International Development Cooperation Agency (SIDA, project number 348-2003-4947), and the Swedish Research Council (project number 621-2007-4124) for financial support.

References:

[1] M.T. Pope, Heteropoly and Isopoly Oxometallates, Springer, Berlin, 1983.

[2] D.E. Katsoulis, Chem. Rev. 98 (1998) 359.

[3] T. Yamase, Chem. Rev. 98 (1998) 307.

[4] M. Sadakane, E. Steckhan, Chem. Rev. 98 (1998) 219.

[5] B. Keita, L. Nadjo, G. Krier, J.F. Muller, J. Electroanal. Chem. 223 (1987) 287.

[6] B. Keita, L. Nadjo, J. Electroanal. Chem. 243 (1988) 87.

[7] B. Keita, L. Nadjo, J. Electroanal. Chem. 247 (1988) 157.

[8] S. Changqing, Z. Jidong, Electrochim. Acta 43 (1998) 943.

[9] L. Qian, X. Yang, Electrochem. Commun. 7 (2005) 547.

[10] S. Dong, B. Wang, Electrochim. Acta 37 (1992) 11.

[11] C. Rong, F.C. Anson, Anal. Chem. 66 (1994) 3124.

[12] A. Kuhn, F.C. Anson, Langmuir 12 (1996) 5481.

[13] L. Cheng, L. Niu, J. Gong, S. Dong, Chem. Mater. 11 (1999) 1465.

[14] Z. Tang, S. Liu, E. Wang, S. Dong, Langmuir 16 (2000) 4946.

[15] Y. Li, W. Bu, L. Wu, C. Sun, Sensor Actuat. B Chem. 107 (2005) 921.

[16] W. Song, Y. Liu, N. Lu, H. Xu, C. Sun, Electrochim. Acta 45 (2000) 1639.

[17] S. Gaspar, L. Muresan, A. Patrut, I.C. Popescu, Anal. Chim. Acta 385 (1999) 111.

[18] G.L. Turdean, A. Curulli, I. Catalin Popescu, C. Rosu, G. Palleschi, Electroanalysis 14 (2002) 1550.

[19] P.J. Kulesza, M. Skunik, B. Baranowska, K. Miecznikowski, M. Chojak, K. Karnicka, E. Frackowiak, F. Béguin, A. Kuhn, M.-H. Delville, B. Starobrzynska, A. Ernst, Electrochim. Acta 51 (2006) 2373.

[20] P. Wang, X. Wang, L. Bi, G. Zhu, J. Electroanal. Chem. 495 (2000) 51.

[21] H.T. Liu, P. He, Z.Y. Li, C.Y. Sun, L.H. Shi, Y. Liu, G.Y. Zhu, J.H. Li, Electrochem. Commun. 7 (2005) 1357.

[22] H. Hamidi, E. Shams, B. Yadollahi, F.K. Esfahani, Talanta 74 (2008) 909.

[23] H. Hamidi, E. Shams, B. Yadollahi, F.K. Esfahani, Electrochim. Acta 54 (2009) 3495.

[24] H. Ji, L. Zhu, D. Liang, Y. Liu, L. Cai, S. Zhang, S. Liu, Electrochim. Acta 54 (2009) 7429.

[25] S. Iijima, Nature 354 (1991) 56.

[26] C.N.R. Rao, B.C. Satishkumar, A. Govindaraj, M. Nath, ChemPhysChem 2 (2001) 78.

[27] F. Valentini, A. Amine, S. Orlanducci, M.L. Terranova, G. Palleschi, Anal. Chem. 75 (2003) 5413.

[28] J.J. Gooding, Electrochim. Acta 50 (2005) 3049.

[29] D. Pan, J. Chen, W. Tao, L. Nie, S. Yao, J. Electroanal. Chem. 579 (2005) 77.

[30] D. Pan, J. Chen, W. Tao, L. Nie, S. Yao, Langmuir 22 (2006) 5872.

[31] J. Qu, X. Zou, B. Liu, S. Dong, Anal. Chim. Acta 599 (2007) 51.

[32] Y. Song, E. Wang, Z. Kang, Y. Lan, C. Tian, Mater. Res. Bull. 42 (2007) 1485.

[33] X. Li, Q. Zhu, S. Tong, W. Wang, W. Song, Sensor Actuat. B Chem. 136 (2009) 444.

[34] A.K. Cuentas-Gallegos, M. Miranda-HernЈndez, A. Vargas-Ocampo, Electrochim. Acta 54 (2009) 4378.

[35] A. Salimi, A. Korani, R. Hallaj, R. Khoshnavazi, H. Hadadzadeh, Anal. Chim. Acta 635 (2009) 63.

[36] M. Skunik, P.J. Kulesza, Anal. Chim. Acta 631 (2009) 153.

[37] J.-f. Liu, G.-b. Jiang, J.-f. Liu, J.A. Jonsson, TrAC, Trends Anal. Chem. 24 (2005) 20.

[38] S. Pandey, Anal. Chim. Acta 556 (2006) 38.

[39] D. Wei, A. Ivaska, Anal. Chim. Acta 607 (2008) 126.

[40] B.Q. Huang, L. Wang, K. Shi, Z.X. Xie, L.S. Zheng, J. Electroanal. Chem. 615 (2008) 19.

[41] L. Wang, Z.-g. Feng, H.-n. Cai, J. Electroanal. Chem. 636 (2009) 36.

[42] J.D. Wadhawan, U. Schr.der, A. Neudeck, S.J. Wilkins, R.G. Compton, F. Marken, C.S. Consorti, R.F. de Souza, J. Dupont, J. Electroanal. Chem. 493 (2000) 75.

[43] H. Chen, Y. Wang, Y. Liu, Y. Wang, L. Qi, S. Dong, Electrochem. Commun. 9 (2007) 469.

[44] Y. Liu, L. Huang, S. Dong, Biosens. Bioelectron. 23 (2007) 35.

[45] N. Maleki, A. Safavi, F. Tajabadi, Anal. Chem. 78 (2006) 3820.

[46] S. Xiaodong, Z. Hongfang, Z. Jianbin, Electrochem. Commun. (2008) 1140.

[47] M.M. Musameh, R.T. Kachoosangi, L. Xiao, A. Russell, R.G. Compton, Biosens. Bioelectron. 24 (2008) 87.

[48] B. Haghighi, H. Hamidi, Electroanalysis 21 (2009) 1057.

[49] R.T. Kachoosangi, M.M. Musameh, I. Abu-Yousef, J.M. Yousef, S.M. Kanan, L. Xiao, S.G. Davies, A. Russell, R.G. Compton, Anal. Chem. 81 (2009) 435.

[50] C.L. Zhou, Y.X. Zheng, Z.Y. Li, Z. Liu, Y.M. Dong, X. Zhang, Electrochim. Acta 54 (2009) 5909.

[51] M.H. Chiang, J.A. Dzielawa, M.L. Dietz, M.R. Antonio, J. Electroanal. Chem. 567 (2004) 77.

[52] J. Zhang, A.M. Bond, D.R. MacFarlane, S.A. Forsyth, J.M. Pringle, A.W.A. Mariotti, A.F. Glowinski, A.G. Wedd, Inorg. Chem. 44 (2005) 5123.

[53] L. Wang, Z.G. Feng, H.N. Cai, J. Electroanal. Chem. 636 (2009) 36.

[54] M. Goral, T. McCormac, E. Dempsey, D.L. Long, L. Cronin, A.M. Bond, Dalton. Trans. (2009) 6727.

[55] J.G. Huddleston, H.D. Willauer, R.P. Swatloski, A.E. Visser, R.D. Rogers, Chem. Commun. (1998) 1765.

[56] A.J. Bard, L.R. Faulkner, Electrochemical Methods, Fundamentals and Applications, Wiley, New York, 2001.

[57] P. Wang, X.P. Wang, G.Y. Zhu, Electroanalysis 12 (2000) 1493.

[58] Z. Li, J. Chen, D. Pan, W. Tao, L. Nie, S. Yao, Electrochim. Acta 51 (2006) 4255.

[59] E. Laviron, J. Electroanal. Chem. 101 (1979) 19.

[60] P. Wang, X.P. Wang, X.Y. Jing, G.Y. Zhu, Anal. Chim. Acta 424 (2000) 51.

[61] P.T. Kissinger, C.R. Preddy, R.E. Shoup, W.R. Heineman, Laboratory Techniques in Electroanalytical Chemistry, Marcel Dekker, New York, 1996.

[62] X.L. Wang, Q. Zhang, Z.B. Han, E.B. Wang, Y.Q. Guo, C.W. Hu, J. Electroanal. Chem. 563 (2004) 221.

[63] D. Martel, A. Kuhn, Electrochim. Acta 45 (2000) 1829.

[64] P. Brimblecombe, in: C.N. Hewitt, A. Jackson, (Eds.) The Handbook of Atmospheric Sciences, Blackwell Science, 2003, Ch. 8, pp. 211.

[65] C.M. Welch, C.E. Banks, A.O. Simm, R.G. Compton, Anal. Bioanal. Chem. 382 (2005) 12.

[66] W.H. Glaze, Environ. Sci. Technol. 21 (1987) 224.

[67] G.L. Kok, T.P. Holler, M.B. Lopez, H.A. Nachtrieb, M. Yuan, Environ. Sci. Technol. 12 (1978) 1072.

[68] R.C. Matos, J.J. Pedrotti, L. Angnes, Anal. Chim. Acta 441 (2001) 73.

[69] A.Y. Tamine, R.K. Robinson, Yogurt Science and Technology, vol. 36, Pergamon, Oxford, 1985, pp. 206.

[70] J. Wang, Y.H. Lin, L. Chen, Analyst 118 (1993) 277.

[71] F.C. Wang, R. Yuan, Y.Q. Chai, D.P. Tang, Anal. Bioanal. Chem. 387 (2007) 709.

[72] Z. Galus, Fundamentals of Electrochemical Analysis, Ellis Horwood Press, New York, 1976.

[73] A.G. Gilman, L.S. Goodman, T.W. Rad, F. Murad, The Pharmacological Basis of Therapeutics, Macmillan, New York, 1985.

[74] J. Jakmunee, K. Grudpan, Anal. Chim. Acta 438 (2001) 299.

[75] J. Liu, L. Cheng, B. Liu, S. Dong, Electroanalysis 13 (2001) 993.

Legends to figures:

Fig. 1. SEM images of GCE/MWCNTs (a), GCE/MWCNTs/$[C_8Py][PF_6]$ (b), and GCE/MWCNTs/$[C_8Py][PF_6]$-PMo_{12} (c). Scale bar: 500 nm; acceleration voltage: 15 kV.

Fig. 2. A) Cyclic voltammograms for a bare GCE (a), GCE/MWCNTs (b) and GCE/MWCNTs/$[C_8Py][PF_6]$ (c) in a solution of 5 mM $K_3Fe(CN)_6$ and 0.1 M KCl at a scan rate of 50 mV s^{-1}. B) Nyquist plots of EIS for a bare GCE (d), GCE/MWCNTs (e) and GCE/MWCNTs/$[C_8Py][PF_6]$ (f) in a solution containing 5 mM $Fe(CN)_6]^{4-/3-}$ couple and 0.1 M phosphate buffer pH of 7.

Fig. 3. Cyclic voltammograms for a GCE/MWCNTs/$[C_8Py][PF_6]$-PMo_{12} (a), GCE/MWCNTs/$[C_8Py][PF_6]$ (b), GCE/MWCNTs/PMo_{12} (c) and GCE/$[C_8Py][PF_6]$-PMo_{12} (d) in 0.5 M H_2SO_4 solution at a scan rate of 50 mV s^{-1}.

Fig. 4. Cyclic voltammograms of a GCE/MWCNTs/$[C_8Py][PF_6]$-PMo_{12} in 0.5 M H_2SO_4 at scan rates of 10 to 1000 mV s^{-1} from inner to outer (a). Plot of peak current density of redox pair II-II' versus scan rate (b) and versus the square root of scan rate (c).

Fig. 5. Cyclic voltammograms of a GCE/MWCNTs/$[C_8Py][PF_6]$-PMo_{12} in 0.5 M H_2SO_4 at different pHs (from a to e: 1.03, 1.49, 1.98, 2.51 and 3.04) and at a scan rate 50 mV s^{-1}. Inset: Variation of potentials as a function of pH for three redox pairs I- I′, II-II′ and III-III′.

Fig. 6. Cyclic voltammograms of a GCE/MWCNTs/$[C_8Py][PF_6]$-PMo_{12} in the presence of 0.0 (a), 5 (b), 10 (c), 20 (d) mM H_2O_2. Inset: cyclic voltammograms of a GCE/MWCNTs/$[C_8Py][PF_6]$ in the absence (e) and in the presence of 1 mM H_2O_2 (f). Supporting electrolyte: 0.5 M H_2SO_4 solution (pH 1.09); potential scan rate: 10 mV s^{-1}.

Fig.7. Cyclic voltammograms of a GCE/MWCNTs/$[C_8Py][PF_6]$-PMo_{12} in the presence of 0.0 , 0.5, 1, 2, 3 and 5 mM iodate (from inner to outer). Inset: cyclic voltammograms of a GCE/MWCNTs/$[C_8Py][PF_6]$ in the absence (g) and in the presence of 1 mM iodate (h). Supporting electrolyte: 0.5 M H_2SO_4 solution (pH 2.56); potential scan rate: 10 mV s^{-1}.

Fig. 8. Hydrodynamic amperometric responses for a GCE/MWCNTs/$[C_8Py][PF_6]$-PMo_{12} to successive additions of 0.02, 0.1 and 1 mM H_2O_2 (from top to down) (a). Plot of amperometric current densities versus H_2O_2 concentrations (b). The recorded chronoamperogram for 100 μM H_2O_2 during long period time (c), Supporting electrolyte: 0.5 M H_2SO_4 solution (pH 1.09); operating potential: -100 mV versus Ag|AgCl|KCl_{sat}; rotating speed: 2000 rpm.

Table 1. Electrochemical characteristics for the various modified electrodes

Electrode	$E°'=1/2\ (E_{pa}+E_{pc})$ *(mV)*			$\Delta E_p=E_{pa}-E_{pc}$ *(mV)*			*Current density*
	I-I′	II-II′	III-III′	I-I′	II-II′	III-III′	*($\mu A\ cm^{-2}$)*
GCE/$[C_8Py][PF_6]$-PMo_{12}	345	192	-71	53	37	35	19.9
GCE/MWCNTs/PMo_{12}	350	198	-28	16	10	11	75.7
GCE/MWCNTs/$[C_8Py][PF_6]$-PMo_{12}	335	191	-64	6	10	6	118.3

Table 2. Analytical parameters for several POM-modified electrodes for hydrogen peroxide and iodate determination.

Electrode	*Type of POM*	*Modification method*	*Electrolyte*	*Analyte*	*Potential (mV)*	*Sensitivity ($\mu A\ mM^{-1}$)*	*LDR (mM)*	*LOD (μM)*	*Reference*
GCE	$CoW_{11}Co$	TiO_2/PVP/ $CoW_{11}Co$	pH 1	IO_3^-	-500	n.d.	0.002-0.28	0.8	[15]
Pt	$PMo_{12}O_{40}^{3-}$	Doped in sol gel film	0.5 M H_2SO_4	H_2O_2	0	3.6	0.02-30	7	[16]
Graphite electrode	$PFeW_{11}O_{39}^{4-}$	Doped in polymer film	pH 2	H_2O_2	0	4.8	Up to 6.5	NR	[17]
Graphite electrode	$H_4Fe_4(PMo_9O_{34})_2^{6-}$	Doped in conducting polymer	pH 6.5	H_2O_2	-40	0.11	Up to 50	2000	[18]
CCE	$P_2W_{17}VO_{62}^{7-}$	Bulk	0.5 M H_2SO_4	IO_3^-	435	0.753	0.1-20	40	[20]
CPE	$PW_{12}O_{40}^{3-}$	Bulk	pH 1	IO_3^-	-100	0.432	0.005-1	3.1	[22]
CPE	$PFeW_{11}O_{39}^{4-}$	Bulk	pH 2	H_2O_2	0	0.183	0.01-0.2	7.4	[23]
ILCPE	$VMo_{12}O_{40}^{3-}$	Bulk	pH 4	H_2O_2	-450	50.83	0.05-2	2.33	[24]
CILE	$PMo_{12}O_{40}^{3-}$	Bulk	pH 2.56	IO_3^-	80	6.3	0.01-1	2.6	[48]
ITO	polymer of $Mo_5P_2O_{23}^{4-}$	Reconstructed by electrolyzing in IL	0.5 M H_2SO_4	IO_3^-	408	NR	NR	NR	[53]
GCE	$P_2W_{18}O_{62}^{6-}$	Multilayer assembly	pH 2.4	IO_3^-	-210	NR	0.003-0.15	3	[75]
GCE	$PMo_{12}O_{40}^{3-}$	MWCNTs/$[C_8Py]$-PMo_{12}	pH 1 pH 2.59	H_2O_2 IO_3^-	-100 0	5.68 14.81	0.02-8 0.02-2	12 15	This work

LDR. linear dynamic range; LOD, limit of detection; NR, not recorded.

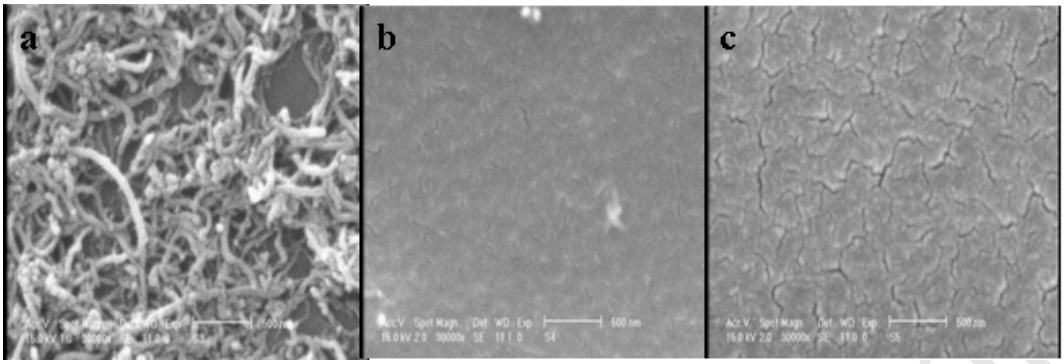

Fig. 1.

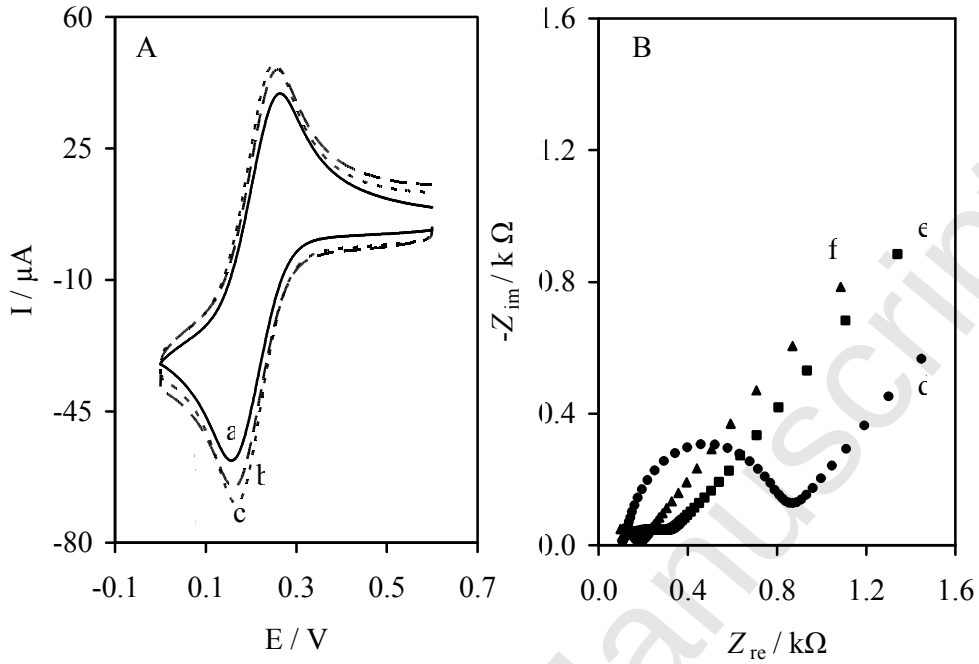

Fig. 2.

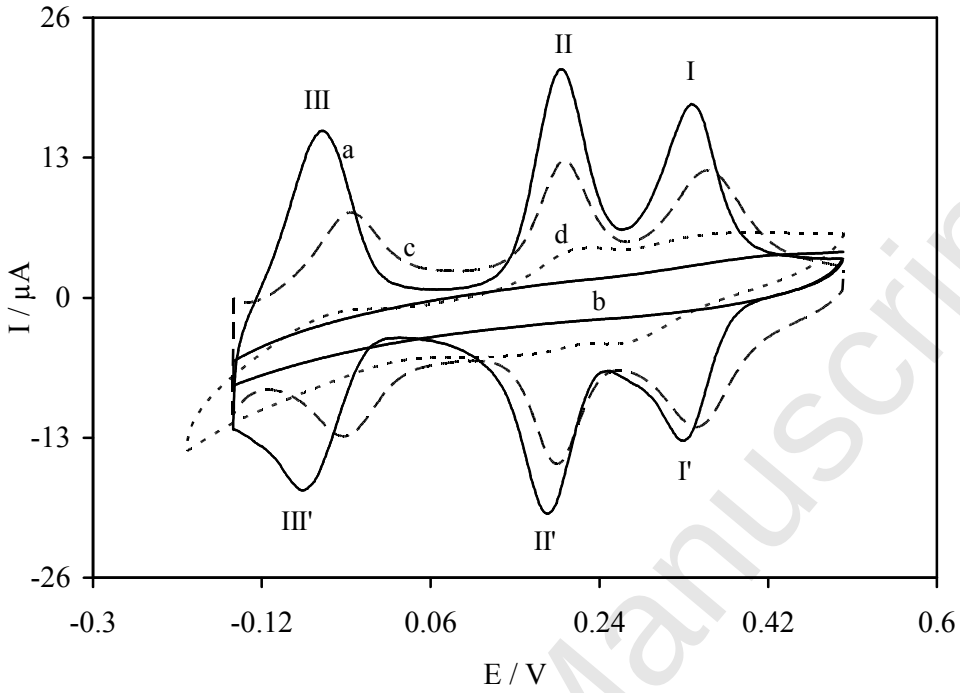

Fig. 3.

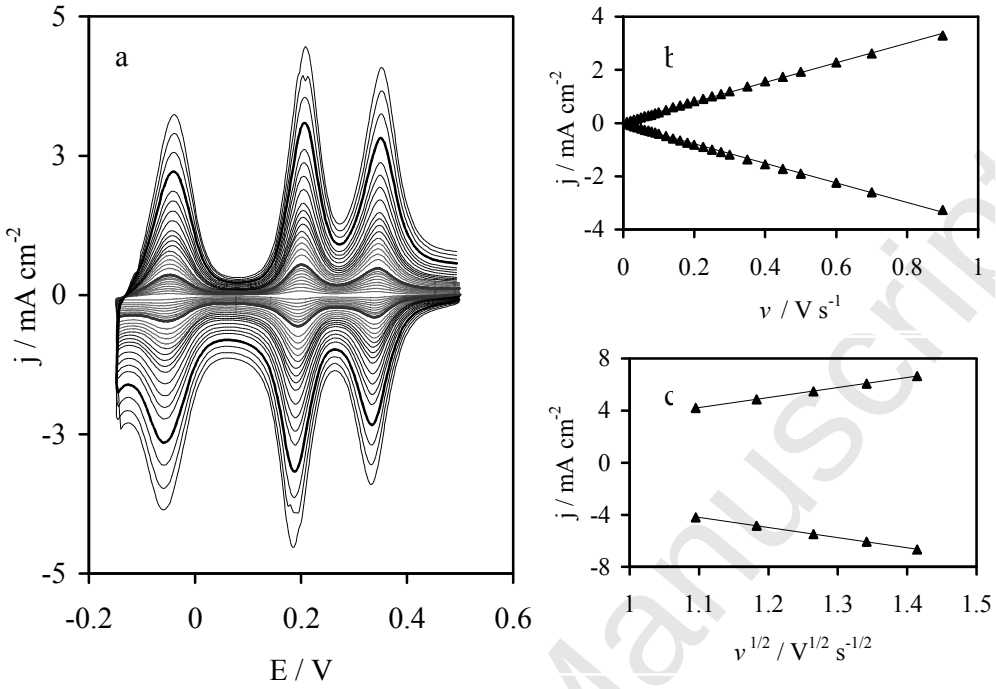

Fig. 4.

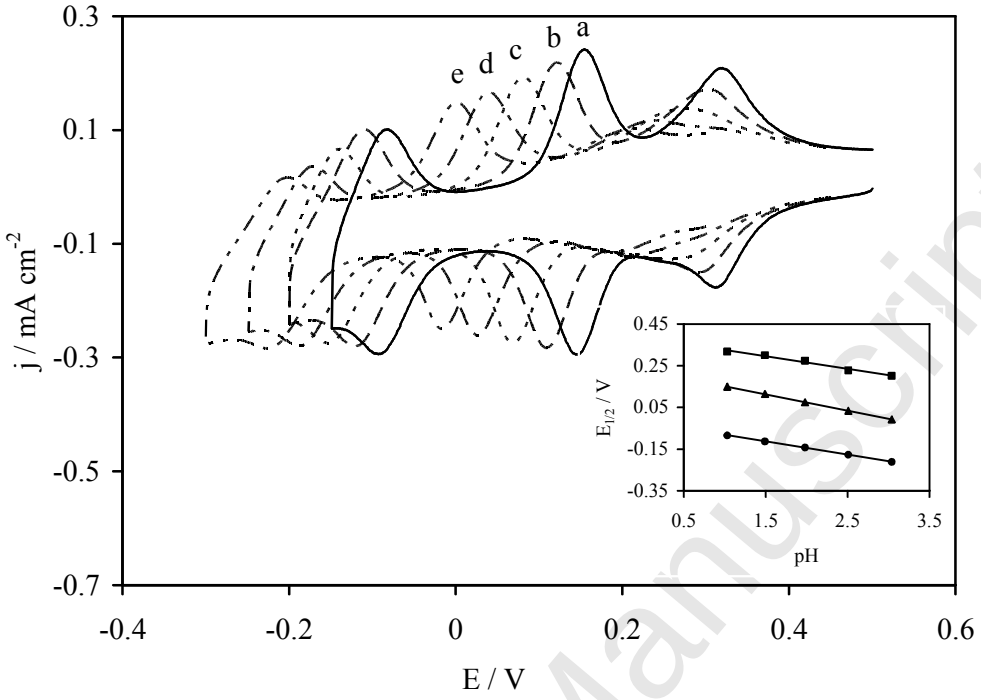

Fig. 5.

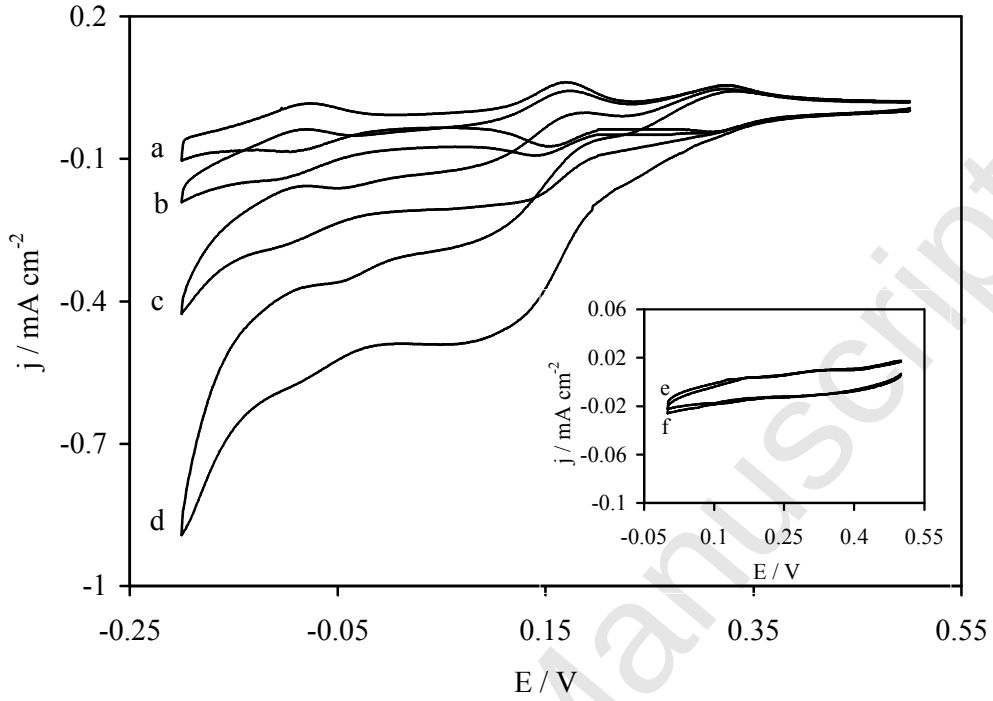

Fig. 6.

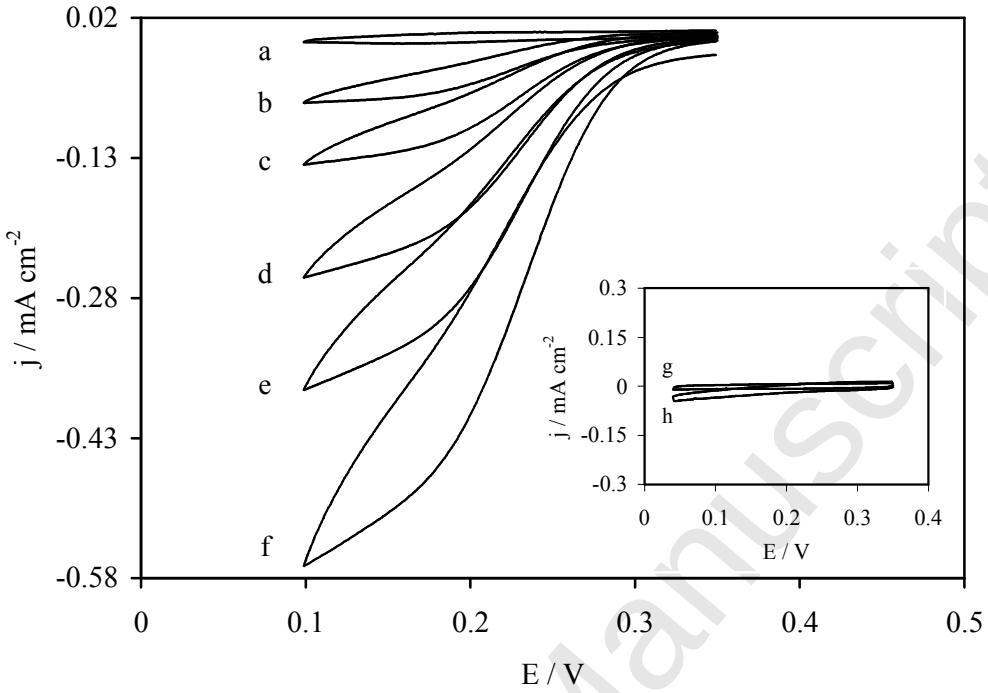

Fig. 7.

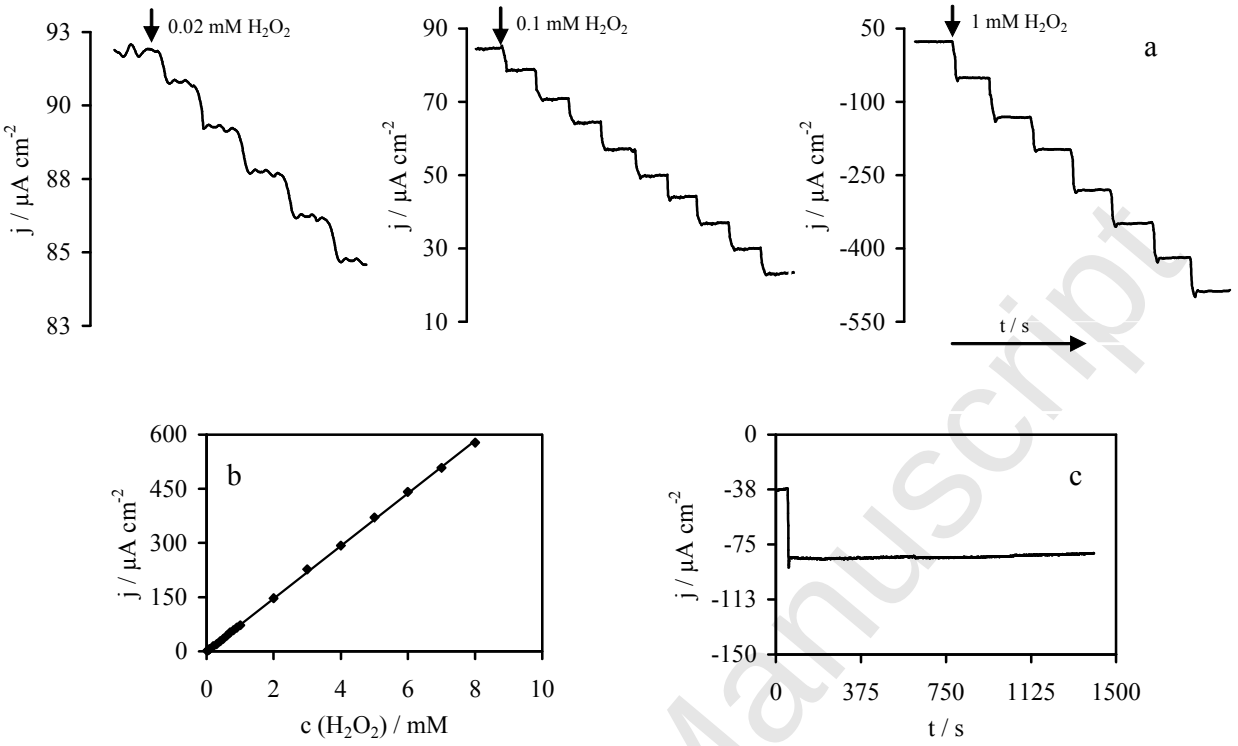

Fig. 8